Biogeosciences Discuss., https://doi.org/10.5194/bg-2019-150
Manuscript under review for journal Biogeosciences
Discussion started: 21 May 2019

Long-term trends in pH in Japanese coastal waters

Miho Ishizu[1], Yasumasa Miyazawa[1], Tomohiko Tsunoda[2], Tsuneo Ono[3]

[1]E-mail: mishizu@jamstec.go.jp

[1]E-mail: miyazawa@jamstec.go.jp

Japan Agency for Marine-Earth Science and Technology, Environmental Variability Prediction and Application Research Group, Yokohama Institute for Earth Sciences, 3173-25 Showa-machi, Kanagawa-ku, Yokohama 236-0001, Japan

Tel: +81-45-778-5875

Fax: +81-45-778-5497

[2]E-mail: t-tsunoda@spf.or.jp

The Ocean Policy Research Institute of the Sasakawa Peace Foundation, 1-15-16, Toranomon Minato-ku, Tokyo 105-8524, Japan

[3]E-mail: tono @affrc.go.jp

Japan Fisheries Research Education Agency, 15F Queen's Tower B, 2-3-3 Minato Mirai, Nishi-ku, Yokohama, Kanagawa 220-6115, Japan

Abstract

In recent decades, acidification of the open ocean has shown consistent increases. However, analysis of long-term data in coastal waters shows that the pH is highly variable because of coastal processes and anthropogenic carbon inputs. It is therefore important to understand how anthropogenic carbon inputs and other natural or anthropogenic factors influence the temporal trends in pH in coastal waters. Using water quality data collected at 1481 monitoring sites as part of the Water Pollution Control Program, we determined the long-term trends in pH in Japanese coastal waters at ambient temperature from 1978 to 2009. We found that pH decreased (i.e., acidification) at between 70% and 75% of the sites and increased (i.e., basification) at between 25% and 30% of the sites. The rate of decrease varied seasonally and was, on average, -0.0014 yr^{-1} in summer and -0.0024 yr^{-1} in winter, but with relatively large deviations from these average values. While the overall trends reflect acidification, watershed processes might also have contributed to the large variations in pH in coastal waters. The seasonal variation in the average pH trends reflects variability in warming trends, while regional differences in pH trends are partly related to heterotrophic water processes induced by nutrient loadings.

Keywords: Ocean acidification, Coastal acidification/basification, pH, Data analysis, CO_2

1. Introduction

The effect of ocean acidification on several marine organisms, including calcifiers, is widely acknowledged and is the topic of various marine research projects worldwide. Chemical variables related to carbonate cycles are monitored in several ongoing ocean projects to determine whether the rate of ocean acidification can be identified from changes in pH and other variables in the open ocean (Gonzalez-Davila et al. 2007; Dore et al. 2009; Bates 2007; Bates et al. 2014; Midorikawa et al. 2010; Olafsson et al. 2009; Wakita et al. 2017). Analysis of pH data measured *in situ* at the European Station in the Canary Islands (ESTOC) in the North Atlantic from 1995 to 2003 and normalized to 25°C showed that pH_{25} decreased at a rate of 0.0017 ± 0.0005 yr^{-1} (Gonzalez-Davila et al. 2007). Similarly, analysis of the Hawaii Ocean Time-series (HOT) (Dore et al. 2009) and the Bermuda Atlantic Time Series (BATS) (Bates 2007) showed that pH at ambient sea surface temperature (pH_{insitu}) decreased by 0.0019±0.0002 and 0.0017±0.0001 yr^{-1} from 1988 to 2007 and from 1983 to 2005, respectively. Analysis of data collected along the hydrographic observation line at 137°E in the western North Pacific by the Japanese Meteorological Agency (JMA) showed that pH_{25} decreased by 0.0013±0.0005 yr^{-1} in summer and 0.0018±0.0002 yr^{-1} in winter from 1983 to 2007 (Midorikawa et al. 2010). The winter pH_{insitu} in surface water in the Nordic Seas decreased at a rate of 0.0024±0.0002 yr^{-1} from 1985 to 2008 (Olafsson et al. 2009). This rate was somewhat more rapid than the average annual rates calculated for the other subtropical time-series stations in the Atlantic Ocean, BATS, and ESTOC, and was attributed to the air–sea CO_2 flux and buffering capacity (higher Revell factor) (Olafsson et al. 2009), which were higher and lower than those in subtropical regions, respectively. Wakita et al. (2017) estimated that the annual and winter pH_{insitu} at station K2 in the subarctic western North Pacific decreased at rates of 0.0025 and 0.0008 yr^{-1}, respectively, from 1999 to 2015. The lower rate in winter

Biogeosciences Discuss., https://doi.org/10.5194/bg-2019-150
Manuscript under review for journal Biogeosciences
Discussion started: 21 May 2019

was explained by increases in dissolved inorganic carbon (DIC) and total alkalinity (Alk) that resulted from climate-related variations in ocean currents.

These long-term time-series from various sites in the open ocean indicate consistent changes in surface ocean carbon chemistry, which mainly reflect the uptake of anthropogenic CO_2, with consequences for ocean acidity. Coastal waters, however, differ from the open ocean as they are subjected to multiple influences, such as hydrological processes, land use in watersheds, nutrient inputs (Duarte et al. 2013), changes in the structure of ecosystems caused by eutrophication (Borges and Gypens 2010; Cai et al. 2011), marine pollution (Zeng et al. 2015), and variations in salinity (Sunda and Cai 2012).

Duarte et al. (2013) hypothesized that anthropogenic pressures would cause the pH_{insitu} of coastal waters to decrease (acidification) or increase (basification), depending on the balance between the atmospheric CO_2 inputs and watershed exports of alkaline compounds, organic matter, and nutrients. For example, in Chesapeake Bay, trends in pH_{insitu} have shown temporal variations over the last 60 years, presumably because of the combined influence of increases and decreases in pH_{insitu} in the mesohaline and polyhaline regions of the mainstem of the bay, respectively (Waldbusser et al. 2011; Duarte et al. 2013). The pH_{insitu} in Tampa Bay increased consistently until 1980 but then dropped almost instantly, only to gradually increase again (Duarte et al. 2013). The increases in pH_{insitu} until 1980 coincided with rapid increases in the population of the Tampa Bay watershed. In this period, nutrients were not stripped from wastewater (Greening and Janicki 2006). However, a nutrient

Biogeosciences Discuss., https://doi.org/10.5194/bg-2019-150
Manuscript under review for journal Biogeosciences
Discussion started: 21 May 2019

management plan was implemented in 1980, and wastewater nutrient-removal was initiated. The sharp decrease in pH_{insitu} throughout the bay at this time might have been related to the decrease in primary production triggered by the reduction in nutrients. In the period after 1980, pH_{insitu} might have increased again because of the expansion of seagrasses, improvements in water quality, and enhanced CO_2 uptake (Duarte et al. 2013).

These processes that occur only in coastal regions might cause increases or decreases in the rate of acidification, meaning that the outcomes for coastal ecosystems in different regions will vary. At present we have limited information about long-term changes in pH in coastal waters, mainly because of the difficulty involved in collecting continuous long-term data from coastal waters around an entire country at a spatial resolution that is sufficient to cover the high regional variability in coastal pH.

The Water Pollution Control Law (WPCL) was established in 1970 to deal with the serious pollution of the Japanese aquatic environment in the 1950s and 1960s. Several environmental variables, including pH_{insitu}, have been continuously measured in coastal waters since 1978, using consistent methods enacted in the monitoring program, to help protect coastal water and groundwater from pollution and retain the integrity of water environments. The errors in pH measurements collected in this program were assessed as outlined in the JIS Z8802 (JIS; Japanese Industrial Standard) standard protocol (2011) that corresponds to the ISO 10523 (ISO; International Organization for Standardization) standard protocol. Compared with the specialized oceanographic protocols described in the United States Department of Energy (DOE) Handbook (1994), it is not difficult to achieve the

Biogeosciences Discuss., https://doi.org/10.5194/bg-2019-150
Manuscript under review for journal Biogeosciences
Discussion started: 21 May 2019

JIS protocol. The JIS and DOE standard protocols allow measurement errors of less than ±0.07 and ±0.003, respectively, for the glass electrode method, and the DOE protocol demands a precision of ±0.001 for the spectrophotometric method. Measurements are generally made with the higher-quality spectrophotometric method during major oceanographic studies (e.g. Midorikawa et al. 2010). The coastal monitoring program in Japan comprises more than 2000 monitoring sites that cover most parts of the coastline (Fig. 1), so the dataset provides the opportunity to estimate the overall trend in pH in Japanese coastal areas and the regional variability in the trends from data with a known precision.

In the present study, we examined the pH_{insitu} trends in surface coastal waters from data measured as part of WPCL monitoring programs. We then examined the trends at specific locations. The remainder of this manuscript is organized as follows. The data and methods are described in Section 2, and trends in pH_{insitu} are presented in Section 3. The results are discussed in Section 4 and the concluding remarks are provided in Section 5.

2. Materials and Methods

2.1 Water Pollution Control Law (WPCL) monitoring data

Data for several environmental variables, including pH_{insitu}, and the associated metadata, are available on the website of the National Institute for Environmental Studies (www.nies.go.jp/igreen; http://www.nies.go.jp/igreen/md_down.html). We downloaded data for pH from 1978 to 2009 for the trend analysis. We also downloaded temperature (T) and total nitrogen (TN) data that were measured at the same sites as the pH data for the same time period (data for T and TN were available from 1981 and 1995, respectively), to check the quality of the pH_{insitu} data (Section 2.2), and to discuss coastal processes that influenced the pH_{insitu} (Section 4.2).

The data were collected by the Regional Development Bureau of the Ministry of Land, Infrastructure, Transport and Tourism, and the Ministry of the Environment under the WPCL monitoring program. Monitoring protocols (sampling frequencies, locations, and methods) are outlined in the program guidelines (NIES 2018; MOE 2018) written in Japanese, and here we summarize that protocols.

Monitoring operations are occupied at 1481 sites along the Japan coast shown in Figure 1a. In each monitoring sites, basic surveys were held 4 to 40 times a year dependent to the site. Information on the sampling frequency at the monitoring sites is presented in Table 1. At each basic survey, water samples were collected at several depths (0.5 and 2.0 m below the surface for all sites, and 10 m where bottom depth was more than this) four times a day to cover diurnal variation. At sites where large variation is found in the daily pH data, additional one day water sampling at 2-hourly intervals (ca. 13 times a day) was made at least twice a year to check the adequacy of basic water sampling protocol.

Measurements of pH for each water sample were made following the Japanese Industrial Standard protocol JIS Z 8802 (2011), which is equivalent to ISO10523 (https://www.iso.org/standard/51994.html). Namely, pH was measured by glass electrode calibrated by NBS standard buffers. Permitted repeatability in each measurement was ±0.07. NIES gathered all

Biogeosciences Discuss., https://doi.org/10.5194/bg-2019-150
Manuscript under review for journal Biogeosciences
Discussion started: 21 May 2019

pH data measured at each site and calculated annual minimum and maximum pH.

The published WPCL pH dataset only contains these annual minimum and maximum pH data, reported on the NBS pH scale (pH_{insitu}) and rounded to one decimal place. Water temperature data are also available for each sampling event (http://www.nies.go.jp/igreen/md_down.html). Previous studies have reported negative correlations between seasonal variations in pH and water temperature, mainly because of changes in the dissociation constant; the pH values were lowest in summer and highest in winter, in both the open ocean (e.g. Bates et al. 2014) and coastal waters (e.g., Frankignoulle and Bouquegneau 1990; Byrne et al. 2013; Hagens et al. 2015; Challener at al. 2016). We therefore assumed that the minimum and maximum pH data coincided with the highest and lowest temperatures, respectively (Fig. 2), and we used these data to calculate pH_{25} in Section 4.2.

The monitoring operations were carried out by licensed operators as outlined in the annual plan of the Regional Development Bureau of each prefecture. These specific licensed operators were retained for the duration of the measurement period, which means that the same laboratories were always in charge of collecting the data. This approach helps to prevent systematic errors that might arise both between measurement facilities and over time, and ensures the datasets are accurate.

2.2 Quality control procedures and assessing the consistency of the WPCL monitoring data

We used all the data for fixed sites that had continuous time-series from 1978 to 2009. There were 2463 regular and non-regular monitoring sites in 1978 and 2127 sites in 2009. While there were few sites in some prefectures in Hokkaido and Tohoku, the monitoring sites covered almost all the coastline in Japan (Fig. 1).

As explained in more detail later in this section, we applied a three-step quality control procedure. We excluded 1) discontinuous time sequences, 2) time sequences that had extreme outliers in each year, and 3) time sequences that included significant random errors and which were only weakly correlated with time sequences at adjacent sites.

When we excluded the sites that had discontinuous time sequences of pH_{insitu} from 1978 to 2009, 1481 sites remained (Fig. 1). We then excluded time sequences with outliers, defined as sites with data points that were more than three standard deviations from the mean for each year. After this step, 1127 sites remained (not shown). We calculated the trends in the unbroken continuous time sequences of the minimum and maximum pH_{insitu} data at each site with linear regression (Fig. 3), and the slopes of the linear regression were taken as the minimum and maximum pH_{insitu} trends (e.g. Fig. 3). The linear regression trends might have been influenced by random errors or variations at different temporal scales in the data for each site. To eliminate the influence of these errors and variations as far as possible, we removed the data that had significant random errors, defined as the time sequences for which the standard deviations of pH_{insitu} exceeded the average standard deviation of the pH_{insitu} time sequences at the 1127 sites. After this step, 302 sites remained (see Fig. 1b for site locations). As shown in Table 2, the correlations between temperature and pH_{insitu} at sites that were within 15 km of each other strengthened after steps 2 and 3, which suggests that the reliability of the dataset improved at each step of the quality control. The mutual correlations among the pH_{insitu} and temperature measurements at adjacent sites (Table 2), and the correlations between pH_{insitu} and TN (Table 3) show that the quality control procedures were effective.

For the 302 sites, we calculated the correlations between water temperature (Fig. 4a–b) and pH_{insitu} (Fig. 4c–d) between pairs of adjacent sites (Fig. 4). At most of the stations, the correlations between the temperatures at the site pairs were relatively strong, which indicates that the temperature followed similar patterns over time at adjacent sites (Fig. 4a–b). The correlations tended to be strong when the sites were close together, but gradually weakened with increasing distance between sites. The patterns in the pH_{insitu} and temperature correlations were similar (Fig. 4c–d), which indicates that the pH_{insitu} and temperature data at adjacent monitoring sites varied in the same way. In other words, the relative ratios of the measurement errors in pH_{insitu} and the natural spatio-temporal variations at these monitoring sites were similar to those for temperature. The absolute values of the pH_{insitu} correlation coefficients were slightly lower than those for temperature for each corresponding pair of sites (Figs. 4 and 5), and might reflect the fact that pH_{insitu}, but not the water temperature, is subjected to strong forcing by coastal biological processes, which causes short-term variations in pH_{insitu}. The correlations between the minimum pH_{insitu} data were weaker than those for the maximum pH_{insitu} data because the degree of biological forcing varied by season and was stronger in summer when pH_{insitu} was at a minimum and weaker in the winter when pH_{insitu} was at a maximum. Despite the influence of biological processes on pH_{insitu}, the correlation coefficients remained high and were significant ($\boldsymbol{r}$=0.367, p<0.05) at most of the monitoring sites, especially at sites that were less than 5 km apart within the same prefecture; at such sites, pH_{insitu} followed similar patterns. In the final step of the quality check procedure (step 3), we removed all the time sequences with weak and insignificant correlations for temperature and pH_{insitu} (Figs. 4 and 5). After this final step, 289 sites remained.

The monitoring in each prefecture is carried out by different licensed operators, decided by the Regional Development Bureau in each prefecture. Even though all the operators follow the same JIS protocol, manual monitoring can introduce systematic errors into the data. Some adjacent monitoring sites are close to each other but are managed by different operators, such as sites close to the boundaries between Osaka and Hyogo, Hyogo and Okayama (Fig. 6), Kagawa and Okayama (not shown), and Kagawa and Ehime (not shown). The pH_{insitu} time sequences for these site pairs were generally similar, even though there were some deviations when compared with the time sequences for adjacent sites within the same prefecture, monitored by the same operator (lines of the same color in Fig. 6). The standard deviations of the pH_{insitu} trends between these site pairs close to the boundaries of Osaka and Hyogo, Hyogo and Okayama, Kagawa and Okayama, and Kagawa and Ehime were 0.0014, 0.0012, 0.0026, and 0.0017 yr^{-1}, respectively, and were smaller than the acceptable measurement errors of the JIS standard protocols. We can therefore say that the measurements from the different operators in different prefectures were consistent.

3. Results

Biogeosciences Discuss., https://doi.org/10.5194/bg-2019-150
Manuscript under review for journal Biogeosciences
Discussion started: 21 May 2019

3.1 Variations in pH_{insitu} highlighted by regression analysis

The histograms of the calculated pH_{insitu} trends (yr^{-1}), for the minimum and maximum pH_{insitu} after each quality control step, are shown in Fig. 7. The histogram in Fig. 7a–b shows data of the 1481 sites (discontinuous sites excluded). The data for 1127 sites (i.e., data without outliers from step 2) are shown in Fig. 7c–d, and the data for 289 sites (from step 3) are shown in Fig. 7e–f (Section 2.2). The number of sites decreased at each step of the quality control, but the shapes of the histograms were generally similar for both the minimum and maximum pH trends. The total trends showed overall normal distributions with a negative shift for all the processing level.

We detected both positive (basification) and negative (acidification) trends, which contrasts with the findings of other researchers who reported only negative trends (ocean acidification) in the open ocean (Bates et al. 2014; Midorikawa et al. 2010; Olafsson et al. 2009; Wakita et al. 2017). The average (± standard deviation) trends for the minimum and maximum pH_{insitu} data were −0.0002±0.0061 and −0.0023±0.0043 yr^{-1} for the 1481 sites (Fig. 7a−b), and −0.0005±0.0042 and −0.0023±0.0036 yr^{-1} for the 1127 sites (Fig. 7c−d), respectively. The average trends for the minimum and maximum pH_{insitu} data for the 289 sites that remained after step 3 were −0.0014±0.0033 and −0.0024±0.0042 yr^{-1}, respectively (Fig. 7e−f).

The negative trends were relatively weak for the minimum pH_{insitu} data and relatively strong for the maximum pH_{insitu} data, but there was an overall tendency towards acidification. The trends that we detected for all the processing levels (Fig. 7) are consistent with, and within the errors of, those reported by Midorikawa et al. (2010), who calculated that pH_{25} decreased at rates of 0.0013±0.0005 yr^{-1} and 0.0018±0.0002 yr^{-1} in summer and winter from 1983 to 2007 along the 137°E line of longitude in the north Pacific.

At the 289 sites, there were 204 negative and 86 positive trends for the minimum pH_{insitu} data and 217 and 72 negative and positive trends for the maximum pH_{insitu} data. This shows that for the minimum data, there were acidification and basification trends at 70% and 30% of the monitoring sites, respectively, with values of 75% and 25% for the maximum data, respectively.

3.2 Local patterns in acidification and basification

We examined the pH_{insitu} trends for the 289 sites for local patterns in acidification and basification (Section 2.2), and found that the trends seemed to be randomly distributed. For example, the values were different at sites that were less than 50 km apart (Fig. 8). There are many monitoring sites in the Seto Inland Sea and in Western Kyushu. The trends for the minimum and maximum pH_{insitu} showed both acidification and basification in the Seto Inland Sea (Fig. 8a–b, 8c–d). In the western part of Kyushu, acidification dominated (Fig. 8a–b, 8c–d) and there were few clusters of basification in pH_{insitu} for both the minimum and maximum pH_{insitu} data (Fig. 8b, d). Figure 8a (b) and Figure 8c (d) are similar, which suggests that, at most of the sites where we detected acidification and basification, the trend directions were consistent for the minimum and maximum pH_{insitu} (Fig. 8a–b, 8c–d).

By examining the average minimum and maximum pH_{insitu} trends in each prefecture (Fig. 9a–b, d–e, g–h, j–k), we found that, while the average values were slightly different, the trends in the averaged values and the patterns in acidification and basification for both the minimum and maximum pH_{insitu} were the same from north to south and from west to east. We also found acidification trends in most of the prefectures with at least 17 sampling sites, namely Miyagi, Wakayama, Hyogo, Okayama, Yamaguchi, Tokushima, Kagawa, Ehime, and Nagasaki (Figs. 1a and 9c, f, i, l). The average estimates for the maximum pH_{insitu} were larger than those for the minimum pH_{insitu} in these prefectures.

We found more acidification trends for the minimum pH_{insitu} in the southwestern prefectures of Yamaguchi, Kagawa, Ehime, Hyogo, and Nagasaki than in the northeastern prefecture of Miyagi (Fig. 9a, d, g, i) (see Fig. 1 for locations). The maximum and minimum pH_{insitu} trends indicated basification in Wakayama and Okayama prefectures (Fig. 9c). The trends in Osaka, Hyogo, Okayama, Hiroshima, Yamaguchi, Kagawa, and Ehime prefectures (Fig. 1a) were different from each other, even though they were all located in the same part of the Seto Inland Sea (Fig. 9d–e). The trends in Hiroshima and Okayama, within the Seto Inland Sea, were weaker than those in Hyogo, Yamaguchi, Kagawa, and Ehime, which were outside the sea (Fig. 9d–e). The pH_{insitu} trend values indicated relatively strong acidification at −0.0025 yr^{-1} in Niigata in the Japan Sea (Fig. 9j–l) but there were fewer than the threshold of 17 monitoring sites in the prefectures.

4. Discussion

4.1 Statistical evaluation of our estimated overall trends

The JIS Z8802 (2011) allows a measurement error of ±0.07 and this treatment further enhanced the uncertainty of the published data to ±0.1. The uncertainty of the slope of the linear regression line (σ_β) is estimated by the following equation (e.g., Luenberger 1969):

$$\sigma_\beta = \{\sigma^2_y / \Sigma(x_i-[x])^2\}^{1/2} \qquad (1)$$

where σ^2_y is theoretical variance in a pH value caused by the measurement error (in this case, $0.1^2 = 0.01$); and x_i and [x] represent the year and the year averaged for all data at a station, respectively. In the WPCL dataset, there are generally 32 data points for each station (for every year from 1978 to 2009), spaced at consistent intervals. In this case, $\Sigma(x_i - [x])^2$ becomes 2728 and σ_β becomes 0.0020 yr^{-1}, which is the threshold of significance for the pH trend. This means that our estimated trends included standard deviations that were less than 0.0020 yr^{-1}, and, if there were no trends, a histogram of pH trends should have a normal distribution with an average and standard deviation (σ_β) of 0.0000 and 0.0020 yr^{-1}, respectively (Fig. 7). The average trend in the maximum pH_{insitu}, however, shifted from zero in a negative direction at a rate of more than 0.0023 yr^{-1} for all three scenarios. This result implies that averaged over the whole country, the Japanese coast was acidified in winter to a degree that could be detected from the historical WPCL pH data, even with an uncertainty of ±0.1. The observed standard deviation for the maximum pH_{insitu} was also larger than the expected value of 0.0020 yr^{-1} because of local variations in the pH trends. The average shift in the minimum pH_{insitu} data was smaller than 0.0020 yr^{-1}, but all three scenarios showed negative shifts in the average minimum pH_{insitu} value (Fig. 7a, c, e).

We used Welch's t test to assess the direction of the average minimum and maximum pH_{insitu} trends. For our null hypothesis, we assumed that the population of the trends with an average of −0.0014 yr^{-1} (−0.0024 yr^{-1}) and a standard deviation of 0.0033 yr^{-1} (0.0042 yr^{-1}) was sampled from a population with an average trend of 0.0000 yr^{-1} and a standard deviation of 0.0020 yr^{-1}. When the sample size was 289, the *t*-values and the degrees of freedom were 8.7 (6.2) and 412.2 (474.4), respectively. Since the p value was less than 0.001, the null hypothesis was rejected. Welch's t test confirmed that the average trends for both the minimum and maximum pH_{insitu} data were negative.

4.2 Possible influences on the pH_{insitu} trends in coastal waters

To facilitate our discussion of the factors that influenced the pH_{insitu} trends, we used the conceptual models of acidification and basification in coastal waters of Sunda and Cai (2012) and Duarte et al. (2013), as follows:

$$PH_{insitu} = \text{Function}\ (D\ (T),\ DIC\ (\text{Air}\ CO_2,\ B\ (T,\ N)),\ Alk(S)) \quad (2)$$

The pH_{insitu} varies with the ambient temperature (T) on seasonal, inter-annual, and decadal time scales mainly because of changes in the water dissociation constant (D). Changes in dissolved inorganic carbon (DIC), alkalinity (Alk), and salinity (S) also affect the pH_{insitu} trends. The solubility pump, which is controlled mainly by the atmospheric CO_2 concentration (Air CO_2), affects DIC, and ocean acidification occurs when the Air CO_2 increases. Dissolved organic carbon can also be affected by biological processes (B) that depend on the ambient temperature (T) and the nutrient loading (N).

There are contrasting relationships between DIC and N in heterotrophic and autotrophic oceans. Because of the balance between primary productivity and respiration in heterotrophic (autotrophic) oceans, the DIC increases as N increases (decreases), causing acidification, but decreases as N decreases (increases), causing basification. Alkalinity (Alk) generally varies with salinity (S) in coastal oceans and might also affect the pH_{insitu} trend.

The DIC process (Air CO_2) of ocean acidification in equation 2 generally occurred at all monitoring sites when the Air CO_2 concentrations were horizontally uniform, resulting in overall negative trends in minimum and maximum pH_{insitu}. D (T) also has an overall trend of warming in Japan coastal area, and hence made some affections to the observed pH_{insitu} trend. We will discuss about this effect in the next chapter.

On the other hand, both DIC (B (T, N)) and Alk (S) are difficult to have general trends that covered all monitoring sites, because factors that control these variables (e.g., salinity of coastal water and terrestrial nutrient loading) have no mutual trends all over the Japan coast. WPCL data contains stations of both autotrophic and heterotrophic oceans, and this condition further obscure affection of DIC (B (T, N)) to overall pH_{insitu} trend, as the same trend of B (T, N) leads opposite trends of DIC (B (T, N) between autotrophic and heterotrophic ocean. Wide-varying nature of D(T), DIC (B (T, N)), and Alk(S) depending on the season and region, however, might have caused the seasonal/regional differences of pH_{insitu} trends among stations, contributing relatively large standard deviations of both the minimum and maximum pH_{insitu} trends (Figures 7).

4.2.1 Seasonal variations in pH_{insitu} trends

Our estimates of the average pH_{insitu} trends show that there was a difference of 0.0010–0.0020 yr^{-1} between the winter and summer trends (Section 3.1, Fig. 7e−f). Our analysis was based on the pH_{insitu} data, so the difference between the trends might reflect long-term changes in water temperature that affected the dissociation constant (process D in equation 2) or changes in the coastal carbon cycle (including absorption of anthropogenic carbon by the solubility pump, represented by DIC in equation 2).

To evaluate the direct thermal effects related to process D in equation 2, we estimated the pH values normalized to 25°C (pH_{25}), assuming that the minimum (maximum) pH_{insitu} and highest (lowest) temperature and other parameters were measured at the same time. By assuming the other parameters that affected the pH calculation in the CO2sys software (Lewis and Wallace 1998, csys.m), such as salinity, DIC, and alkalinity, did not change (these parameters are not measured as part of the WPCL program), we used the method of Lui and Chen (2017) to calculate the pH_{25}, as follows:

$$pH_{25} = -pH_{insitu} + a_1(T - 25°C), \qquad (3)$$

where a_1 is set to −0.015 and T is the observed temperature.

The distributions of the trends in pH_{25} after applying equation 3 are shown in Fig. 10. The minimum and maximum pH_{25} data were normally distributed, meaning that the distributions of the pH_{insitu} trends were maintained after applying equation 3 (Fig. 7e, f). The averages (± standard deviations) of the

Biogeosciences Discuss., https://doi.org/10.5194/bg-2019-150
Manuscript under review for journal Biogeosciences
Discussion started: 21 May 2019

minimum and maximum pH_{25} trends were −0.0010±0.0032 and −0.0014±0.0041 yr^{-1}, respectively, so the average for the minimum and maximum pH_{25} still showed acidification, but the trends were slightly weaker than those for the minimum and maximum pH_{insitu} (−0.001 yr^{-1} less) (Fig. 7e–f).

The pH_{25} and pH_{insitu} trends from north to south and from west to east were similar among the prefectures (Fig. 11), except in Miyagi and Tokushima. The trends in the minimum pH_{insitu} and summer pH_{25} were quite similar, but the minimum and maximum pH_{insitu} trends tended to be more negative (by about −0.0010 yr^{-1}) than the corresponding pH_{25} trends, especially in Wakayama, Hiroshioma, Kagawa, and Ehime, which met the threshold number of sampling sites.

The average highest temperatures observed at the minimum pH_{insitu} were close to 25°C in the regions south of Chiba prefecture (Figs. 1 and 12a–d), so we were not able to remove the thermal effects from the minimum pH_{25} in the southern prefectures. In contrast, the maximum pH_{insitu} values were observed at temperatures that were more than 10°C lower than 25°C, so we were able to normalize the winter data. We estimated the temperature trends from the highest and lowest temperatures at the 289 sites that remained after quality control step 3. The trends in the highest and lowest temperatures generally indicated warming, with an average and standard deviation of 0.021±0.040 and 0.047±0.036 °C yr^{-1}, respectively (Fig. 13). Estimations from the CO2sys software indicate that these warming trends influenced the pH values and were related to the changes of −0.0004 and −0.0010 yr^{-1} in the pH trends in summer and winter, respectively (Fig. 7e–f and 10a–b). We estimated that the pH_{insitu} would change from 8.0150 to 8.0147 in summer and from 8.2560 to 8.2565 in winter, for temperature changes from

Biogeosciences Discuss., https://doi.org/10.5194/bg-2019-150
Manuscript under review for journal Biogeosciences
Discussion started: 21 May 2019

25.00°C to 25.02°C, and from 10.00°C to 10.04°C, respectively, for a salinity of 34, DIC of 1900 millimole m^{-3}, and alkalinity of 2200 millimole m^{-3}. The differences between the pH_{insitu} and the corresponding pH_{25} trends in summer (0.0004 yr^{-1}) and winter (−0.0010 yr^{-1}) can be partly explained by the difference between the decrease in the pH trends in summer (−0.0003 yr^{-1}) and winter (−0.0005 yr^{-1}) (Fig. 7e−f) arising from thermal effects.

4.2.2 Regional differences in pH_{insitu} trends

We found regional differences in pH_{insitu} values (e.g. Fig. 6) and pH_{insitu} trends (Figs. 8−9). The negative pH_{insitu} trends (acidification) were more significant in southwestern Japan than in northeastern Japan, especially for the minimum pH_{insitu} data (Fig. 9 and Section 3.2). The JMA (2008, 2018) reported that over the past 100 years, the increase in water temperature in western Japan was ~1.30°C greater than that in northeastern Japan.

We used the CO2sys software (Lewis and Wallace 1998) to predict how pH_{insitu} would change under a temperature difference of 0.01 °C yr^{-1} between the northeastern and southwestern areas, and found that pH decreased by 0.0002 (0.0002) yr^{-1} when the temperature changed from 10.00°C to 10.01°C (25.0°C to 25.01°C), assuming a salinity of 34, DIC of 1900 millimol/m^3, and alkalinity of 2200 millimol/m^3. The contrasting trends in the northeast and southwest can be also partly explained by the difference in warming trends (process D in equation 2).

Regional differences in pH were observed in the northern Gulf of Mexico and the East China Sea

(Cai et al. 2011) at the basin scale. Yamamoto-Kawai et al. (2015) detected regional differences in the aragonite saturation rate (Ω_{ar}) of an ocean acidification index, but not in pH_{insitu}, in Tokyo Bay. Cai et al. (2011) reported that regional differences in pH_{insitu} observed in their surveys were caused by human-related inputs of nutrients to coastal waters; i.e., eutrophication (represented by the DIC process in equation 2). Sunda and Cai (2012) used biogeochemical simulations to examine the complex interactions between acidification that resulted from respiratory CO_2 inputs and from increasing atmospheric CO_2. With their model, which focused on coastal areas, they predicted that these CO_2 inputs caused pH_{insitu} values to decrease by between 0.1250 and 1.1000 units because of eutrophication. Both Cai et al. (2011) and Sunda and Cai (2012) considered heterotrophic subsurface waters. Spatial variations in nutrient loadings in autotrophic waters also cause pH_{insitu} trends to vary, although in the opposite direction (Borges and Gypens 2010), and eutrophication can result in basification (Duarte et al. 2013).

As well as the effect of changes in the disassociation constant, the summer pH_{insitu} is affected by ocean uptake of CO_2 (process DIC; Bates et al. 2012; Bates 2014) through long-term changes in biological activity (Cai et al. 2011; Sunda and Cai 2012; Duarte et al. 2013; Yamamoto-Kawai et al. 2015). The responses of pH_{insitu} to changes in marine productivity are, however, complicated.

Previous studies have reported that nutrient loadings in Japan have decreased over recent decades (e.g., Yamamoto-Kawai et al. 2015; Kamohara et al. 2018; Nakai et al. 2018), with variable effects on summer pH_{insitu} in coastal waters. TN was monitored for a shorter period than pH_{insitu} (1995 to 2009).

Biogeosciences Discuss., https://doi.org/10.5194/bg-2019-150
Manuscript under review for journal Biogeosciences
Discussion started: 21 May 2019

We assumed that the TN was mainly dissolved inorganic nitrogen, and determined the correlations between TN and the minimum and maximum pH_{insitu} data (Fig. 14). There were significant negative correlations between TN and minimum (−0.03) and maximum (−0.29) pH_{insitu}. These correlations imply that the conditions in most of the monitoring areas of the WPCL programs were heterotrophic. There is little evidence of basification, even in coastal waters, but the heterotrophic coastal waters monitored by the WPCL programs might have been oligotrophic. While some sites might have been dominated by heterotrophs, others might have been affected by autotrophs, causing the dominant processes in the pH trends to vary between sites, depending on the area.

Nakai et al. (2018) reported that nutrient loadings have decreased in the most parts of the Seto Inland Sea from 1981 to 2010, but several areas remain eutrophic. Because of geographical variations in nutrient loadings and the uneven distribution of autotrophic and heterotrophic water areas, there are significant spatial variations in pH trends in the Seto Inland Sea (Fig. 8). The pH trends in coastal areas of western Kyushu, where the anthropogenic nutrient loadings are relatively low, therefore reflect the decreases in nutrient discharges, resulting in variations between regions (e.g., Nakai et al. 2018; Yamamoto and Hanazato 2015; Tsuchiya et al., 2018). Several cities in this area have introduced advanced sewage treatment to prevent eutrophication in coastal waters (Nakai et al. 2018; Yamamoto and Hanazato 2015).

Variations in coastal alkalinity along with salinity might be related to changes in land use and might affect the trends (process Alk(S) in equation 2). Total alkalinity is not monitored as part of the WPCL program and there are no sites in coastal areas of Japan with continuous data for alkalinity. Taguchi et al. (2009) measured alkalinity in the surface waters of Ise, Tokyo, and Osaka bays between 2007 and 2009, and reported that total alkalinity was highly correlated with salinity in each bay. For a temperature, salinity, dissolved carbon, and alkalinity of 25.00 °C, 35, 1900 millimol m^{-3}, and 2300 millimol m^{-3}, respectively, pH_{insitu} (= pH_{25}) was estimated at 8.1416 using the CO2sys software (Lewis and Wallace 1998). By changing the salinity and alkalinity to 34 and 2200 millimol m^{-3}, respectively, pH_{insitu} (= pH_{25}) decreased by 0.0081 to 8.0150. This shows that pH could deviate significantly from average trends if the inputs of alkaline compounds are changed; consequently, some of our pH trends could have been affected by changing discharge from different land-use types.

Regional differences in pH_{insitu} trends in coastal waters might be caused by ocean pollution. The speciation and bioavailability of heavy metals change in acidic waters, causing an increase in the biotoxicity of the metals (Zeng et al. 2015; Lacoue-Labarthe et al. 2009; Pascal et al. 2010; Cambell et al. 2014). The rates at which marine organisms photosynthesize and respire in ocean waters decrease and increase, respectively, in water polluted with heavy metals and oils (process DIC in equation 2) because of biotoxicity and eutrophication, thereby resulting in acidification (Hing et al. 2011; Huang et al. 2011; Gilde and Pinckney 2012).

5. Conclusions

We estimated the long-term trends in pH_{insitu} in Japanese coastal waters and examined how the trends varied regionally. The long-term pH_{insitu} data show highly variable trends, although ocean acidification has generally intensified in Japanese coastal waters. We found that the annual pH_{insitu} minimum (in summer) and pH_{insitu} maximum (in winter) decreased at overall rates of −0.0014 and −0.0024 yr^{-1}, respectively, in Japanese coastal waters, similar to the adjacent open ocean. The seasonal differences in average pH trends might reflect differences in warming trends, and the regional differences in pH trends are partly related to heterotrophic processes associated with nutrient loadings.

There were striking spatial variations in the pH_{insitu} trends. Correlations among the pH_{insitu} time series at different sites revealed that the high variability in the pH_{insitu} trends was not caused by analytical errors in the data but reflected the large spatial variability in the physical and chemical characteristics of coastal environments, such as water temperature, nutrient loadings, and autotropic/heterotrophic conditions. While there was a general tendency towards coastal acidification, there were positive trends in pH_{insitu} at 25%–30% of the monitoring sites, indicating basification, which suggests that the coastal environment might not be completely devastated by acidification. If we can manage the coastal environment effectively (e.g., control nutrient loadings and autotropic/heterotrophic conditions), we might be able to limit, or even reverse, acidification in coastal areas.

Acknowledgments

We thank the scientists, captain, officers, and personnel of the National Institute for Environmental Studies, Regional Development Bureau of the Ministry of Land, Infrastructure, Transport and Tourism, who contributed to this study. We acknowledge financial support from the Sasakawa Peace Foundation of the Ocean Policy Research Institute. We also appreciate discussions with members of the Environmental Variability Prediction and Application Research Group of the Japanese Agency for Marine-Earth Science and Technology. Suggestions by two reviewers helped us to improve an earlier version of the manuscript.

References

Bates, N. R.: Interannual variability of the ocean CO_2 sink in the subtropical gyre of the North Atlantic Ocean over the last 2 decades, J. Geophys. Res. 112, C09013, doi:10.1029/2006JC003759, 2007.

Bates, N. R.: Multi-decadal uptake of carbon dioxide into subtropical mode waters of the North Atlantic Ocean. Biogeosciences 9:2, 649–2, 659, http://dx.doi.org/10.5194/bg-9-2649-2012, 2012.

Bates, N. R., Astor, Y. M., Church, M. J., Currie, K., Dore, J. E., Gonzalez-Davila, M., Lorenzoni, L., Muller-Karger, F., Olafsson, J., and Santana-Casiano, J. M.: A time-series view of changing surface ocean chemistry due to ocean uptake of anthropogenic CO_2 and ocean acidification, Oceanography, 27 (1):126–141, http://dx.doi.org/10.5670/oceanog.2014.16, 2014.

Bednarsek, N., Tarling, G. A., Bekker, D. C. E., Fielding, S., Jones, E. M., Venables, H. J., Ward, P., Kuzirian, A., Leze, B., Feely, R. A., and Murphy, E. J.: Extensive dissolution of live pteropods in the Southern Ocean, Nature Geoscience Letter, 5, 881–885, doi: 10.1038/NGEO1635, 2012.

Bednarsek, N., Feely, R. A., Reum, J. C. P., Peterson, B., Menkel, J., Alin, S. R., and Hales, B.: *Limacina helicina* shell dissolution as an indicator of declining habitat suitability due to ocean acidification in the California Current Ecosystem, Proc. R. Soc. B, 281 20140123, doi:

Biogeosciences Discuss., https://doi.org/10.5194/bg-2019-150
Manuscript under review for journal Biogeosciences
Discussion started: 21 May 2019

10.1098/rspb.2014.0123, 2014.

Borges, A. V. and Gypen, N.: Carbonate chemistry in the coastal zone responds more strongly to eutrophication than to ocean acidification, Limnology and Oceanography 55: 346–353, 2010.

Montagna, R.: Description and quantification of pteropod shell dissolution: a sensitive bioindicator of ocean acidification, Global Change Biology, 18, 2378–2388, doi: 10.1111/j.1365–2486.2012.02668, 2012.

Byrne, M., Lamare, M., Winter, D., Dworjanyn, S. A., and Uthicke, S.: The stunting effect of a high CO_2 ocean on calcification and development in the urchin larvae, a synthesis from the tropics to the poles, Philosophical Transactions of the Royal Society B, 368, 20120439. Doi: 10.1098/rstb.2012.0439, 2013.

Cai ,W., Hu, X., Huang, W., Murell, M. C., Lehrter, J. C., Lohrenz, S. E., Chou, W., Zhai, W., Hollibaugh, J. T., Wang, Y., Zhao, P., Guo, X., Gundersen, K., Dai, M., and Gong, G.: Acidification of subsurface coastal waters enhanced by eutrophication, Nature Geoscience, 4, 766–700, 2011.

Campbell, A. L., Mangan, S., Ellis, R. P., and Lewis, C.: Ocean acidification increases copper toxicity to the early life history stages of the polychaete arenicola marina in artificial seawater, Environ. Sci. Technol. 48, 9745–9753, 2014.

Challener, R. C., Robbins, L. L., and McClintock, J. B.: Variability of the carbonate chemistry in a shallow, seagrass-dominated ecosystem: imprications for ocean acidification experiments, Marine and Freshwater Research, 67, 163-172. Doi:10.1071/MF14219, 2016.

Biogeosciences Discuss., https://doi.org/10.5194/bg-2019-150
Manuscript under review for journal Biogeosciences
Discussion started: 21 May 2019

DOE (United States Department of Energy): Handbook of methods for the analysis of the various parameters of the carbon dioxide system in sea water; ver. 2, edited by A. G. Dickson and C. Goyet, ORNL/CDIAC-74, 1994.

Dore, J. E., Lukus, R., Sadler, D. W., Church, M. J. and Karl. D. M.: Physical and biogeochemical modulation of ocean acidification in the central North Pacific, Proc. Natl. Acad. Sci. 106, 12 235−12 240, 2009.

Doney, S.C., Fabry, V. J., Freely, A., and Kleypas, J. A.: Ocean acidification: The other CO_2 program, Annu. Rev. Mar. Sci, 1, 169−192, 2009.

Duarte, C. M., Hendriks, I. E., Moore, T. S., Olsen, Y. S., Steckbauer, A., Ramajo, L., Carstensen, J., Trotter, J. A., and McCullouch, M.: Is ocean acidification an open ocean syndrome? Understanding anthropogenic impacts in seawater pH, Estuaries and Coasts 36, 221-236.doi:10.1007/s12237-013-9594-3, 2013.

Frankignoulle, M., and Bouquegneau, J. M.: Daily and yearly variations of total inorganic carbon in a productive coastal area, Estuarine, Coastal and Shelf Science 30, 79-89, 1990.

Gattuso, J. P., and Hansson, L.: Ocean acidification, Oxford Univ. Press, Oxford, 2011.

Glide, K., and Pinckney, J. L.: Sublethal effects of crude oil on the community structure of estuarine phytokton, Estuar. Coasts 35, 853−861, 2012.

Gonzalez-Davila, M., Santana-Casiano, J. M., and Gonzalez-Davila, E. F.: Interannual variability of the upper ocean carbon cycle in the northeast Atlantic Ocean, Geophys. Res. Lett. 34, L07608, doi:10.1029/2006GL028145, 2007.

Hagens, M., Slomp, C. P., Meysman, F. J. R., Seitaj, D., Harlay, J., Borges, A. V., and Middelburg, J. J.: Biogeochemical processes and buffering capacity concurrently affect acidification in a seasonally hypoxic coastal marine basin, Biogeoscience 12, 1561-1583. Doi:10.5194/bg-12-1561-2015, 2015.

Hing, L. S., Ford, T., Finch, P., Crane, M., and Morritt, D.: Laboratory stimulation of oil-spill effects on marine phytoplankton, Aquat. Toxicol 103, 32−37, 2011.

Huang, Y. J., Jiang, Z. G., Zeng, J. N., Chen, Q. Z., Zhao, Y. Q., Liao, Y. B., Shou, L., and Xu, X. Q.: The chronic effects of oil pollution on marine phytoplankton in a subtropical bay, China. Environ. Monit. Assess. 176, 517−530, 2011.

Intergovernmental Panel on Climate Change (IPCC): Climate Change 2013: The Physical Science Basis. Contribution of Working Group I to the Fifth Assessment Report of the Intergovernmental Panel on Climate Change, ed. Stocker, T. F., Qin, D., Plattner, Gian-Kasper., Tignor, M. M. B., Allen, S. K., Boschung, J., Nauels, A., Zia Y., Bex, V., Midgley, P. M., 1−1535 pp. Cambridge, UK: Cambridge University Press, Cambridge, United Kingdom and New York, NY, USA, 2013.

Japanese Industrial Standard Z8802 : http://kikakurui.com/z8/Z8802-2011-01.html (in Japanese), 2011.

Japanese Meteorological Agency : http://dl.ndl.go.jp/view/download/digidepo_3011050_po_synthesis.pdf?itemId=info%3Andljp%2Fpid%2F3011050&contentNo=1&alternativeNo=&__lang=en, 2008.

Biogeosciences Discuss., https://doi.org/10.5194/bg-2019-150
Manuscript under review for journal Biogeosciences
Discussion started: 21 May 2019

Japanese Meteorological Agency : https://www.data.jma.go.jp/kaiyou/data/shindan/a_1/japan_warm/japan_warm.html (in Japanese), 2018.

Kamohara, S., Takasu, Y., Yuguchi, M., Mima, N., and Yoshunari, A.: Nutrient decrease in Mikawa Bay, Bulletin of Aichi Fisheries Research Institute 23, 30-32. (in Japanese), 2018.

Keeling, C. D., and Whorf, T. P.: Atmospheric CO_2 concentration–Manoa Loa Observatory, Hawaii, 1958-1997 (revised August 1998), ORNL NDP−001, Oak Ridge Nathl. Lab. Oak Ridge, TN, 1998.

Lacou-Labarthe, T., Martin, S., Oberhansli, F., Teyssie, J. L., Jeffree, R., Gattuso, J. P., and Bustamante, P.: Effects of increased pCO_2 and temperature on tracer element (Ag, Cd and Zn) bioaccumulation in the eggs of the common cuttlefish, Sepia officinalis. Biogeosciences 6, 1−3, 2009.

Lemasson, A. J., Fletcher, S., Hall-Spence, J. M., and Knights, A. M.: Linking the biological impacts of ocean acidification on oysters to changes in ecosystem services: A review, Journal of Experimental Marine Biology and Ecology, 492, 49−62, 2017.

Lewis, E., and Wallace, D. W. R.: Program Developed for CO2 System Calculations. ORNL/CDIAC-105. Carbon Dioxide Information Analysis Center, Oak Ridge National Laboratory, U.S. Department of Energy, Oak Ridge, Tennessee, 1998.

Luenberger, D. G.: Optimization by vector space methods, pp. 1-326, John Wiley & Sons, Inc., New York, N.Y, 1969.

Lui, H., and Chen, A. C.: Reconciliation of pH_{25} and pH_{insitu} acidification rates of the surface oceans: A simple conversion using only in situ temperature, Limnology and Oceanography : methods, 15, 328-355, doi:1002/lom3.10170, 2017.

Midorikawa, T., Ishii, M., Sailto, S., Sasano, D., Kosugi, N., Motoi, T., Kamiya, H., Nakadate, A., Nemoto, K., and Inoue, H.: Decreasing pH trend estimated from 25-yr time series of carbonate parameters in the western North Pacific, Tellus, 62B, 649−659, doi: 10.111/j.1600−0889.2010.00474.x, 2010.

Ministry of the Environment: http://www.env.go.jp/hourei/05/000140.html (in Japanese), 2018.

Nakai, S., Soga, Y., Sekito, S., Umehara, S., Okuda, T., Ohno, M., Nishijima, W., and Asaoka, S.: Historical changes in primary production in the Seto Inland Sea, Japan, after implementing regulations to control the pollutant loads, Water Policy wp2018093. Doi:10.2166/wp.2018.093, 2018.

National Institute for Environmental Studies : https://www.nies.go.jp/igreen/explain/water/content_w.html (in Japanese), 2018.

Olafsson, J., Olafsdottir, S. R., Benoit-Cattin, A., Danielsen, M., Arnarson, T. S., and Takahashi, T.: Rate of Iceland Sea acidification from time series measurements, Biogeosciences 6:2, 661−2, 668, http://dx.doi.org/10.5194/bg−6−2661−2009, 2009.

Pascal, P. Y., Fleeger, J. W., Galvez, F., and Carman, K. R.: The toxicological interaction between ocean acidity and metals in coastal meiobenthic copepods, Mar. Pollut. Bull, 60, 2201−2208, 2010.

Sarmiento, J. L., and Gruber, N.: Ocean Biogeochemical dynamics, pp. 1-503, Princeton Univ. Press,

Biogeosciences Discuss., https://doi.org/10.5194/bg-2019-150
Manuscript under review for journal Biogeosciences
Discussion started: 21 May 2019

Princeton, New Jersey; Oxfordshire, United Kingdom, 2006.

Sunda, W. G., and Cai, W. J.: Eutrophication induced CO_2-acidification of subsurface coastal waters: interactive effects of temperature, salinity, and atmospheric pCO_2, Environ. Sci. Technol. 46, 10651−10659, 2012.

Taguchi, F., Fujiwara, T., Yamada, Y., Fujita, K., and Sugiyama, M.: Alkalinity in coastal seas around Japan, Bulletin on coastal oceanography, Vol.47, No.1, 71−75, 2009.

Yamamoto-Kawai, M., Kawamura, N., Ono, T., Kosugi, N., Kubo, A., Ishii, M., and Kanda, J.: Calcium carbonate saturation and ocean acidification in Tokyo Bay, Japan, J. Oceanogr. 71:427−439, doi 10.1007/s10872-015-0302-8, 2015.

Tsuchiya, K., Ehara, M., Yasunaga, Y., Nakagawa, Y., Hirahara, M., Kishi, M., Mizubayashi, K., Kuwahara, V. S., and Toda, T.: Seasonal and Spatial Variation of Nutrients in the Coastal Waters of the Northern G*oto Islands, Japan, Bulletin on coastal oceanography, 55, 125-138. (in Japanese)*, 2018.

Yamamoto, T., and Hanazato, T.: Eutrophication problems of oceans and lakes, -fishes cannot live in clean water, pp. 1−208, ChijinShokan Co. Ltd, ISBN978-4-8052-0885-4, (in Japanese), 2015.

Yara, Y., Vogi ,M., Fujii, M., Yamano, H., Hauri, C., Steinacher, M., Gruber, N. and Yamano, Y. : Ocean acidification limits temperature-induced poleward expansion of coral habitats around Japan, Biogeosciences, 9, 4955−4968, doi : 10.5194/bg-9-4955-2012, 2012.

Zeng, X., Chen, X., and Zhuang, J.: The positive relationship between ocean acidification and pollution,

Biogeosciences Discuss., https://doi.org/10.5194/bg-2019-150
Manuscript under review for journal Biogeosciences
Discussion started: 21 May 2019

Mar. Poll. Bull, 91, 14−21, 2015.

Wakita, M., Nagano, A., Fujiki, T., and Watanabe, S.: Slow acidification of the winter mixed layer in the subarctic western North Pacific, J. Geophys. Res. Oceans, 122, 6923−6935, doi:10.1002/2017JC013002, 2017.

Biogeosciences Discuss., https://doi.org/10.5194/bg-2019-150
Manuscript under review for journal Biogeosciences
Discussion started: 21 May 2019

Figure captions

Fig. 1 Coastal maps and monitoring sites in Japan. Red points in (a) indicate the fixed sites (n = 1481) monitored by the Regional Development Bureau of the Ministry of Land, Infrastructure, Transport, and Tourism, and the Ministry of the Environment (Japan) under the WCPL monitoring program. (b) Monitoring sites that met the strictest criterion (n = 302).

Fig. 2 Distributions of the monthly number of data points (N) for (a) maximum and (b) minimum temperatures collected in each prefecture from the 302 most reliable monitoring sites.

Fig. 3 Examples of (a) acidification (Kahoku Coast in Ishikawa) and (b) basification (Funakoshi Bay in Iwate) trends at monitoring sites. Red and blue colors indicate the annual minimum and maximum pH_{insitu} data and their trends, respectively.

Fig. 4 Correlations of water temperature and pH_{insitu} at adjacent monitoring sites in the same prefecture. Thin lines denote significant correlations ($\boldsymbol{r}$ = 0.12, degrees of freedom = 283).

Fig. 5 Scatter plots of correlation coefficients for water temperature and pH_{insitu} at adjacent monitoring sites in the same prefecture. Fig. 5a shows the highest temperature and minimum pH_{insitu} data and Fig.

5b shows the lowest temperature and maximum pH_{insitu} data.

Fig. 6 Examples of time-series for annual minimum and maximum pH_{insitu} data at adjacent monitoring sites close to the boundaries between (a) Osaka and Hyogo and (b) Kagawa and Ehime. Lines of the same color indicate data collected at the same site. Site locations are included to the right of each panel, with the text color corresponding to the colors in each panel.

Fig. 7 Histogram of pH trends, represented by ΔpH_{insitu}, showing the slopes of the linear regression lines for the annual minimum (left) and maximum (right) pH_{insitu} data at each monitoring site. The histograms in (a, b), (c, d), and (e, f) show three scenarios: (a, b) all 1481 available sites with continuous records before quality control, (c, d) 1127 sites without outliers, and (e, f) 289 sites that meet the strictest criterion.

Fig. 8 Distributions of long-term trends in pH_{insitu} (ΔpH_{insitu}/yr) in Japanese coastal waters. The colors indicate the ranges of acidification (a, c) and basification (b, d). (a, b) and (c, d) are linked to the data used in Figs. 7e and 7f, respectively.

Fig. 9 (a–b, d–e, g–h, j–k) Average minimum and maximum pH_{insitu} trends (ΔpH_{insitu}/yr) in each prefecture. These figures show each side of the Pacific (a–b), the Seto Inland Sea (d–e), the East

China Sea (g–h), and the Japan Sea (j–k). The prefecture names are arranged vertically from eastern (northern) to western (southern) areas. Black and red shading indicate one standard deviation from the average. (c, f, i, l) Number of monitoring sites in each prefecture. The thin dashed line is the threshold value of 17 (i.e., the average number of monitoring sites in all prefectures). The prefectures that meet the threshold are indicated in purple. The figure is based on the results shown in Figs. 7 (e, f) and 8.

Fig. 10 Same as Fig. 7, but showing the pH_{25} trends at 289 sites (selected by quality control step 3). The value of pH_{25} was estimated using the method of Lui and Chen (2017).

Fig. 11 (a–b, d–e, g–h, j–k) Same as Fig. 9, but showing the average estimated minimum and maximum pH_{25} trends (ΔpH_{25}/yr) for each prefecture. Red lines and points indicate the average minimum and maximum pH_{insitu} trends shown in Fig. 9.

Fig. 12 Average highest and lowest temperatures observed for the minimum and maximum pH_{insitu} data for each prefecture. The blue and red lines and shading indicate the average and one standard deviation from the average, respectively. The prefectures that met the threshold of 17 are shown in purple, as in Figs. 9 (c-l) and 11 (c-l).

Biogeosciences Discuss., https://doi.org/10.5194/bg-2019-150
Manuscript under review for journal Biogeosciences
Discussion started: 21 May 2019

Fig. 13 Same as Fig. 7, but showing the highest and lowest temperature trends at 289 sites (selected by quality control step 3).

Fig. 14 Correlation between trends in total nitrogen (TN) and trends in (a) minimum and (b) maximum pH_{insitu}. The correlation coefficients are −0.30 and −0.29 for the minimum and maximum pH_{insitu}, respectively (significance level of 0.05, $r = 0.128$; degrees of freedom = 236).

Table 1 Number of samples (N) collected at each of the 1481 monitoring sites each year.

Table 2 Average mutual correlation coefficients among water temperature and pH_{insitu} measurements at adjacent monitoring sites in the same prefecture. The averages were calculated from the data for the highest and lowest temperature, and minimum and maximum pH_{insitu} within 15 km for the three criteria. We refined the sites using three quality control steps, yielding 1481 (step 1), 1127 (step 2), and 302 (step 3) sites.

Table 3 Average correlation coefficients of minimum and maximum pH_{insitu} trends with total inorganic nitrogen (TN) trends. The degrees of freedom in steps 1 and 2 are the same values because TN data are not necessarily measured at all pH_{insitu} monitoring sites and the sampling numbers of monitoring sites for steps 1 and 2 are the same.

Biogeosciences Discuss., https://doi.org/10.5194/bg-2019-150
Manuscript under review for journal Biogeosciences
Discussion started: 21 May 2019

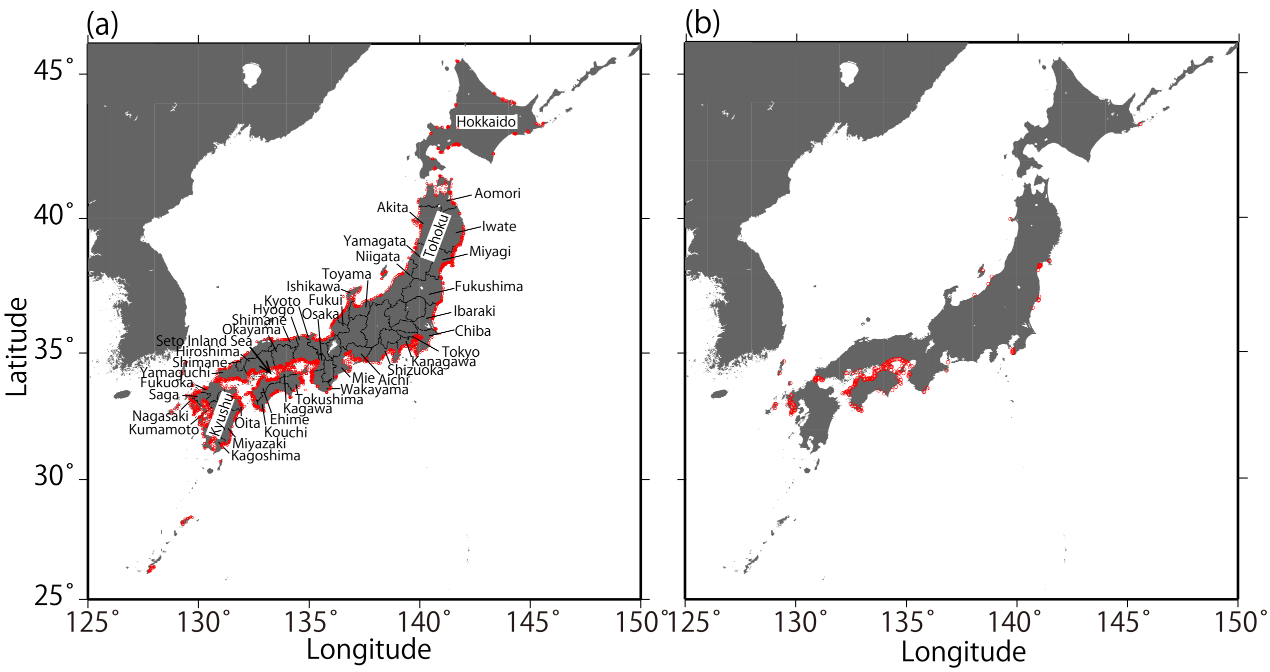

Fig. 1 Coastal maps and monitoring sites in Japan. Red points in (a) indicate the fixed sites (n = 1481) monitored by the Regional Development Bureau of the Ministry of Land, Infrastructure, Transport, and Tourism, and the Ministry of the Environment (Japan) under the WCPL monitoring program. (b) Monitoring sites that met the strictest criterion (n = 302).

Biogeosciences Discuss., https://doi.org/10.5194/bg-2019-150
Manuscript under review for journal Biogeosciences
Discussion started: 21 May 2019

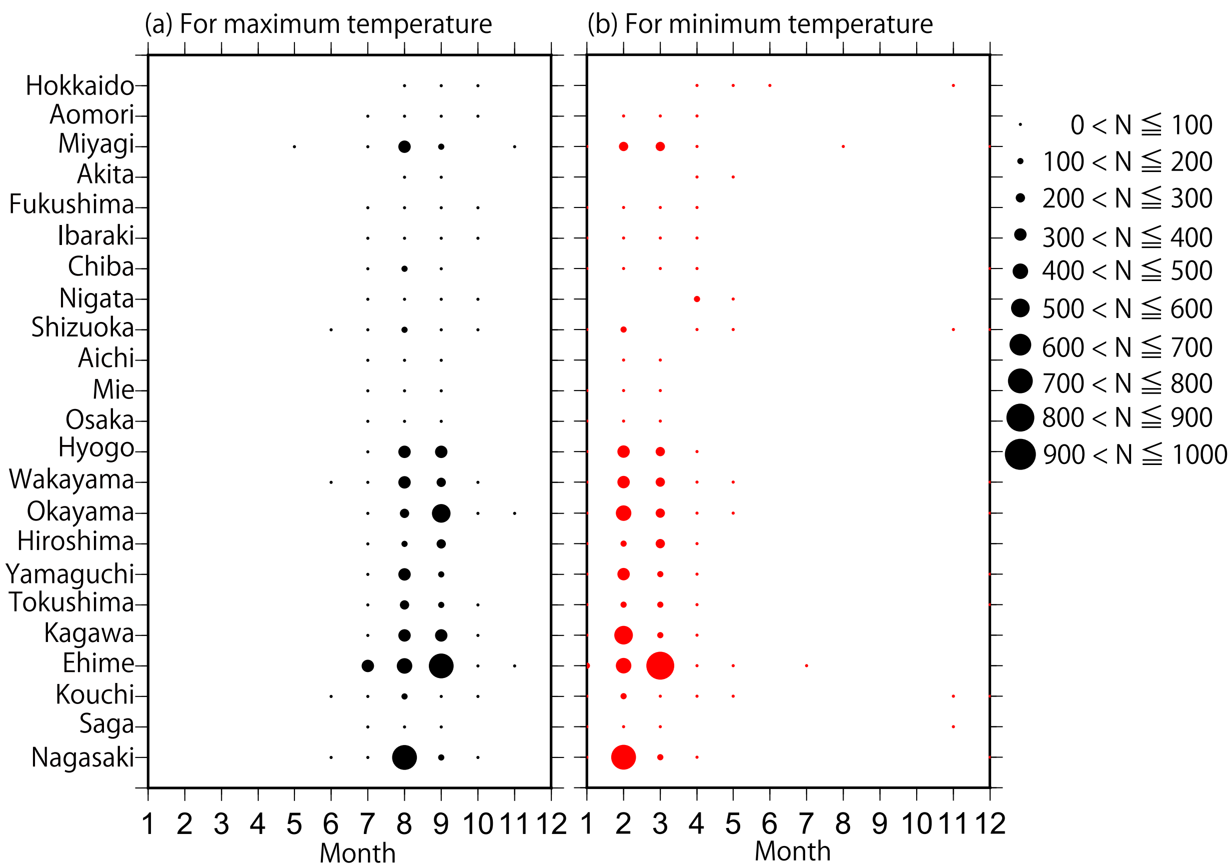

Fig. 2 Distributions of the monthly number of data points (N) for (a) maximum and (b) minimum temperatures collected in each prefecture from the 302 most reliable monitoring sites.

Biogeosciences Discuss., https://doi.org/10.5194/bg-2019-150
Manuscript under review for journal Biogeosciences
Discussion started: 21 May 2019

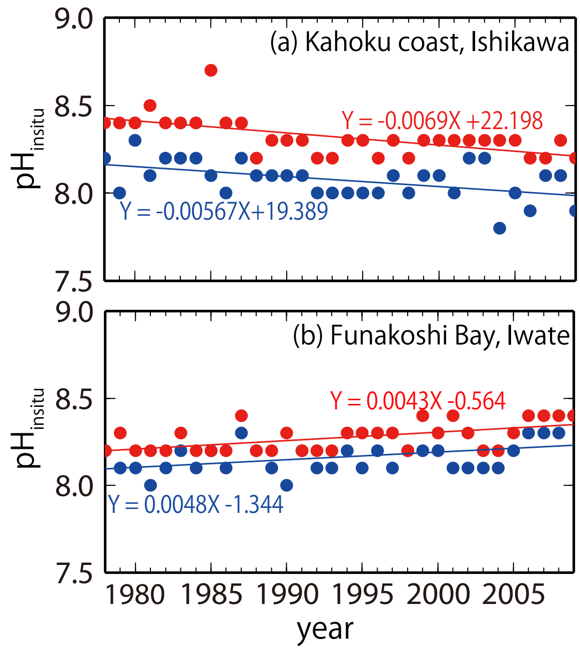

Fig. 3 Examples of (a) acidification (Kahoku Coast in Ishikawa) and (b) basification (Funakoshi Bay in Iwate) trends at monitoring sites. Red and blue colors indicate the annual minimum and maximum pH_{insitu} data and their trends, respectively.

Biogeosciences Discuss., https://doi.org/10.5194/bg-2019-150
Manuscript under review for journal Biogeosciences
Discussion started: 21 May 2019

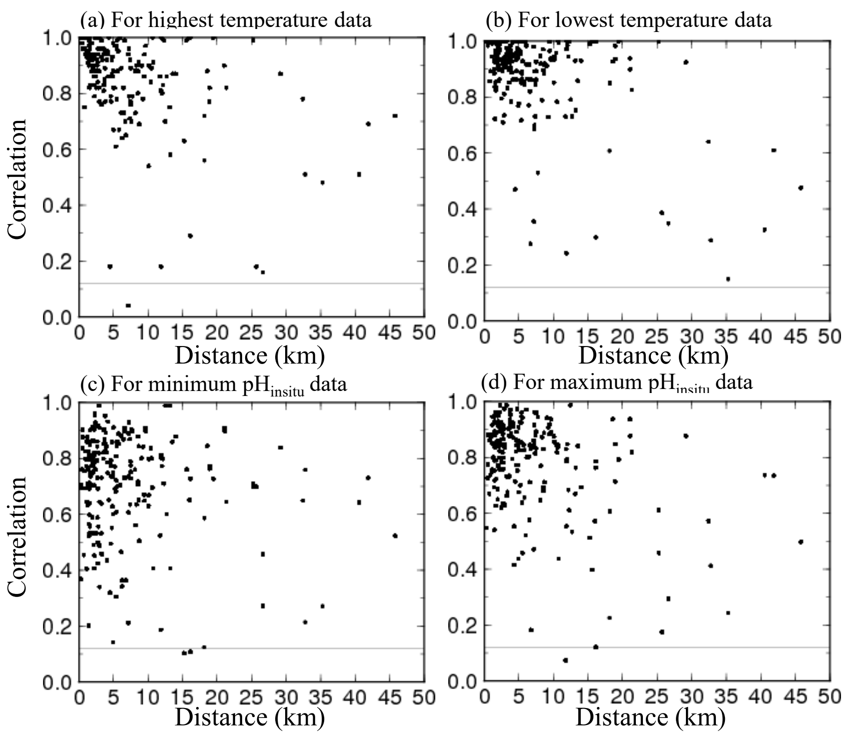

Fig. 4 Correlations of water temperature and pH_{insitu} at adjacent monitoring sites in the same prefecture. Thin lines denote significant correlations (***r*** = 0.12, degrees of freedom = 283).

Biogeosciences Discuss., https://doi.org/10.5194/bg-2019-150
Manuscript under review for journal Biogeosciences
Discussion started: 21 May 2019

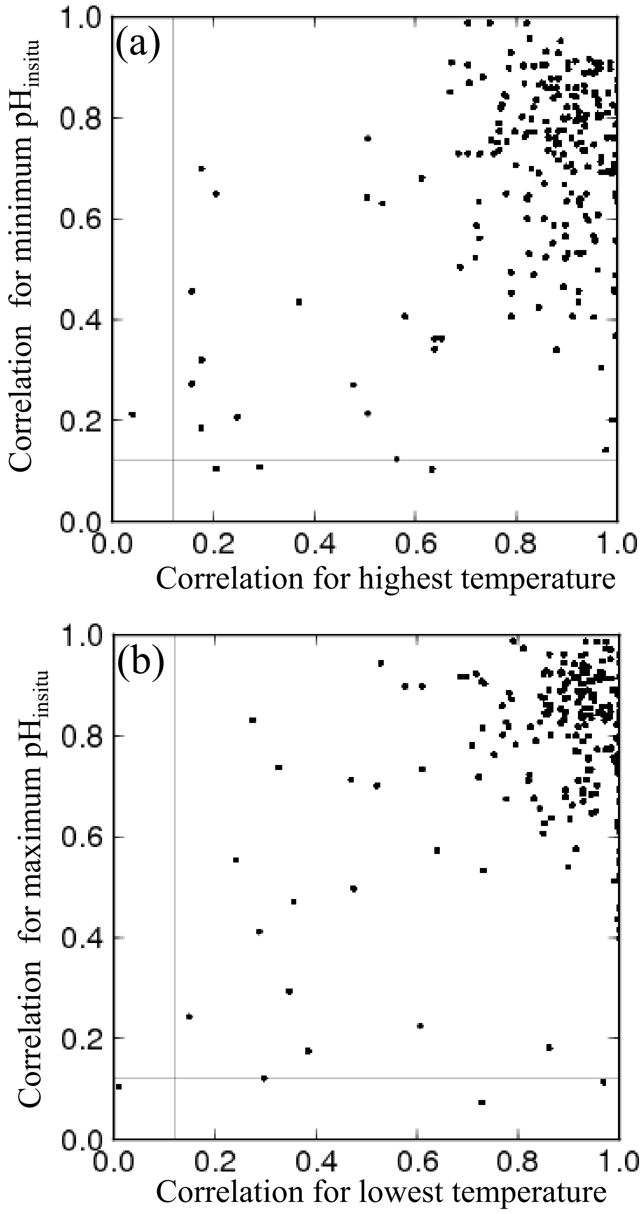

Fig. 5 Scatter plots of correlation coefficients for water temperature and pH_{insitu} at adjacent monitoring sites in the same prefecture. Fig. 5a is for the highest temperature and the minimum $pH_{inisitu}$ data and Fig. 5b for the lowest temperature and the maximum pH_{insitu} data, respectively.

Biogeosciences Discuss., https://doi.org/10.5194/bg-2019-150
Manuscript under review for journal Biogeosciences
Discussion started: 21 May 2019

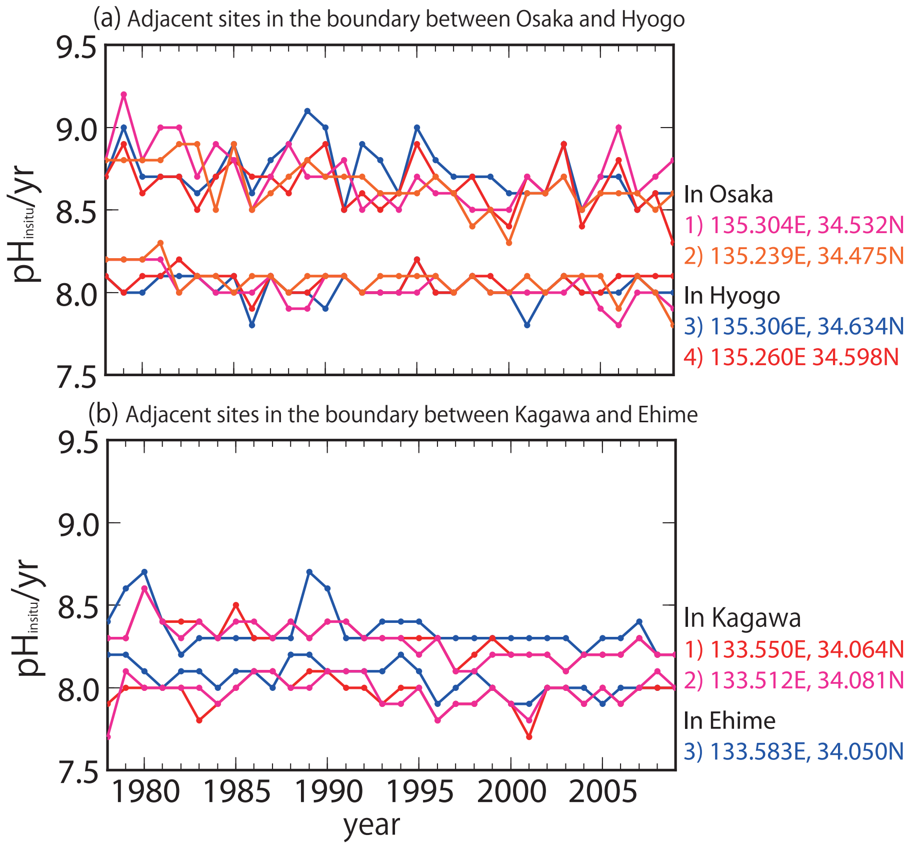

Fig. 6 Examples of time-series for annual minimum and maximum pH_{insitu} data at adjacent monitoring sites close to the boundaries between (a) Osaka and Hyogo and (b) Kagawa and Ehime. Lines of the same color indicate data collected at the same site. Site locations are included to the right of each panel, with the text color corresponding to the colors in each panel.

Biogeosciences Discuss., https://doi.org/10.5194/bg-2019-150
Manuscript under review for journal Biogeosciences
Discussion started: 21 May 2019

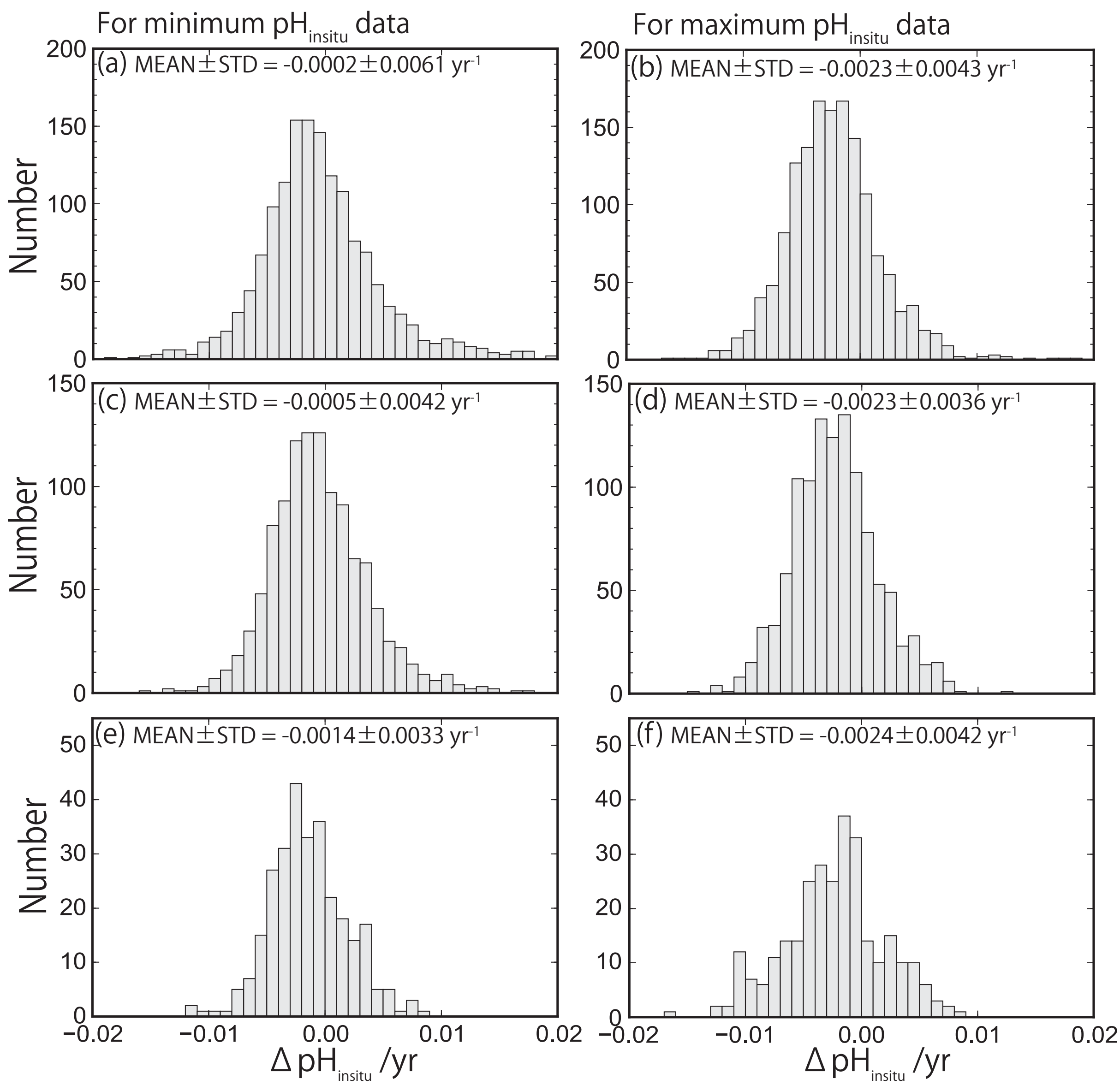

Fig. 7 Histogram of pH trends, represented by ΔpH_{insitu}, showing the slopes of the linear regression lines for the annual minimum (left) and maximum (right) pH_{insitu} data at each monitoring site. The histograms in (a, b), (c, d), and (e, f) show three scenarios: (a, b) all 1481 available sites with continuous records before quality control, (c, d) 1127 sites without outliers, and (e, f) 289 sites that meet the strictest criterion.

Biogeosciences Discuss., https://doi.org/10.5194/bg-2019-150
Manuscript under review for journal Biogeosciences
Discussion started: 21 May 2019

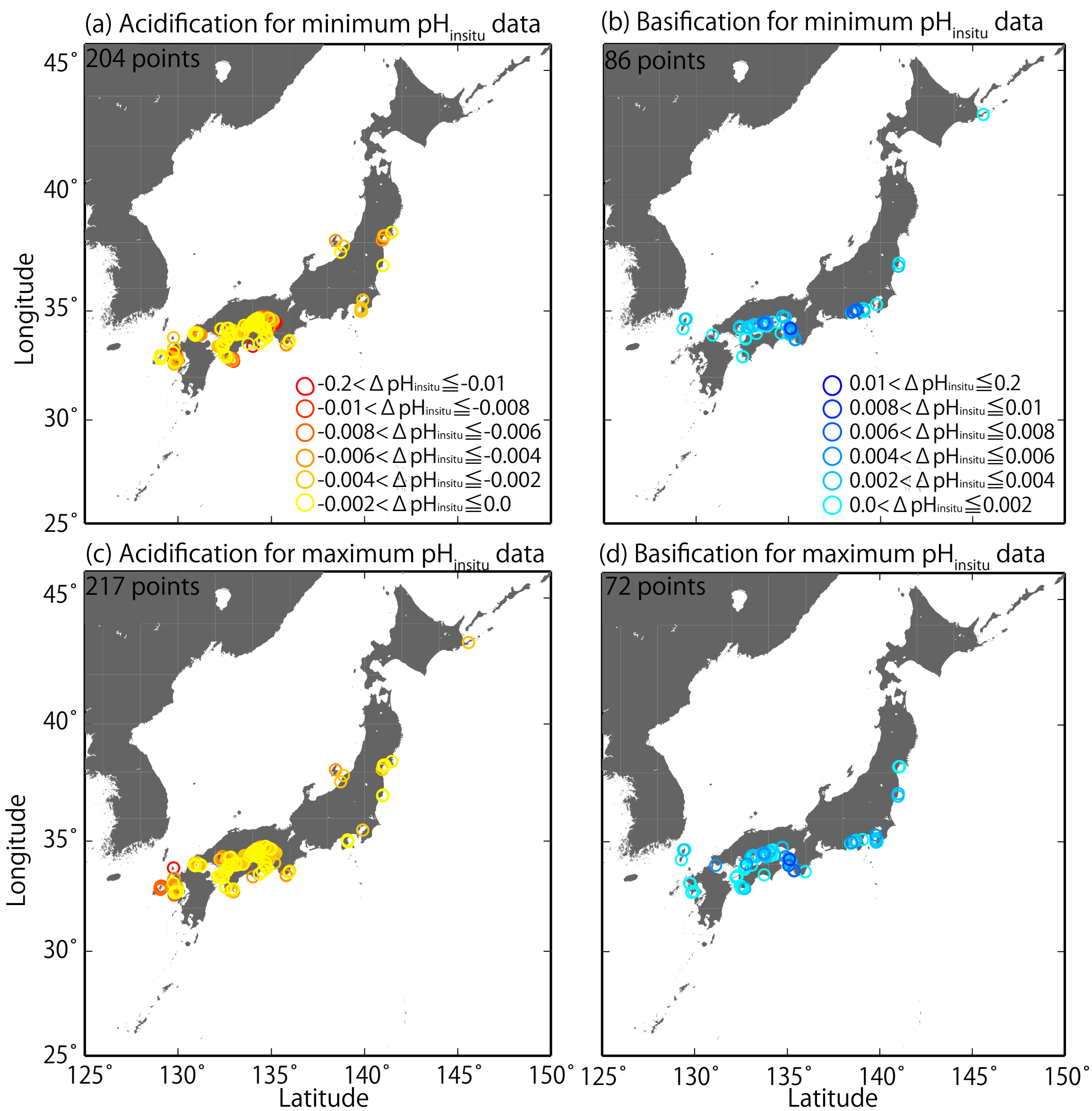

Fig. 8 Distributions of long-term trends in pH_{insitu} (ΔpH_{insitu}/yr) in Japanese coastal waters. The colors indicate the ranges of acidification (a, c) and basification (b, d). (a, b) and (c, d) are linked to the data used in Figs. 7e and 7f, respectively.

Biogeosciences Discuss., https://doi.org/10.5194/bg-2019-150
Manuscript under review for journal Biogeosciences
Discussion started: 21 May 2019

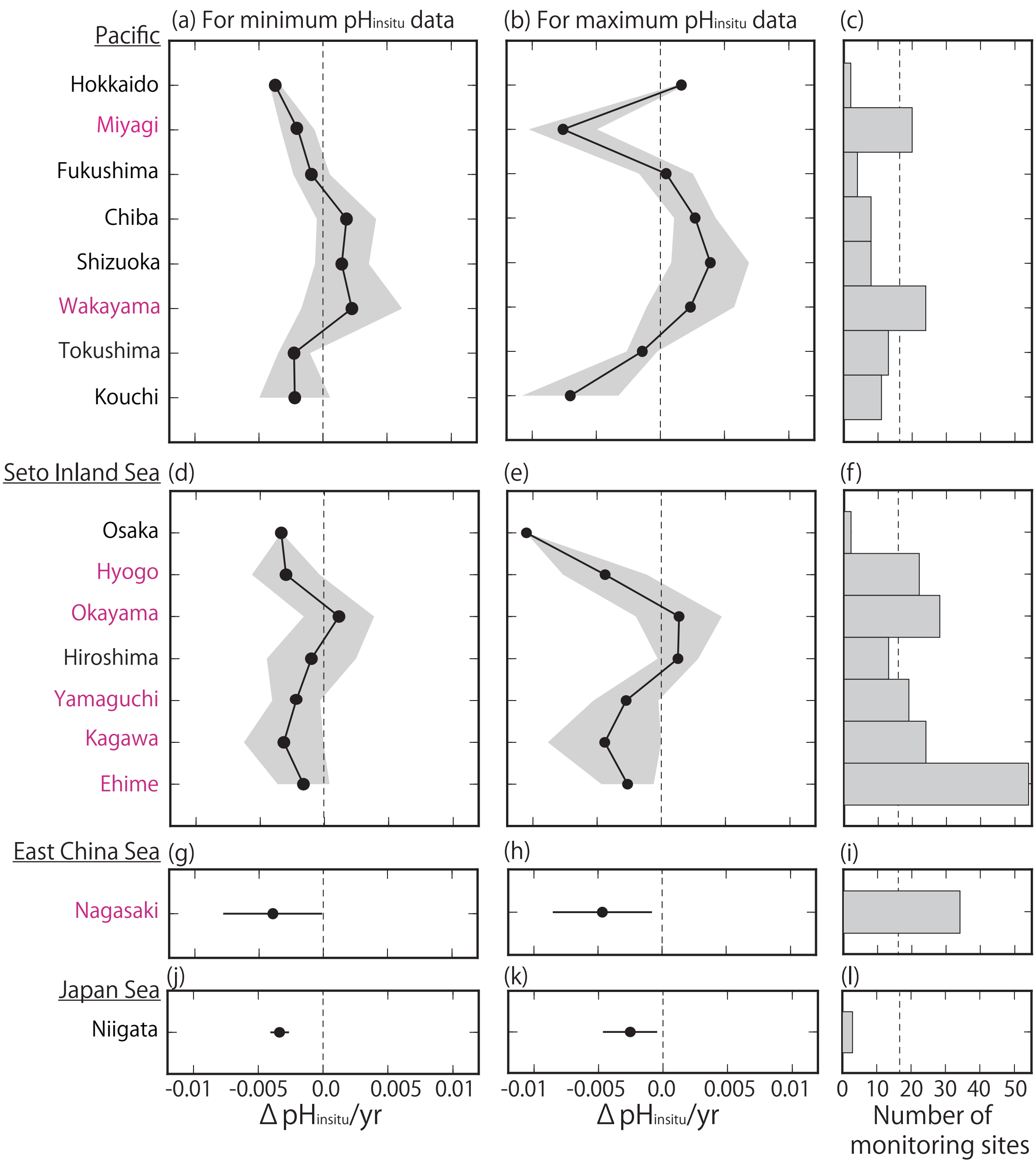

Fig. 9 (a–b, d–e, g–h, j–k) Average minimum and maximum pH_{insitu} trends (ΔpH_{insitu}/yr) in each prefecture. These figures show each side of the Pacific (a–b), the Seto Inland Sea (d–e), the East China Sea (g–h), and the Japan Sea (j–k). The prefecture names are arranged vertically from eastern (northern) to western (southern) areas. Black and red shading indicate one standard deviation from the average. (c, f, i, l) Number of monitoring sites in each prefecture. The thin dashed line is the threshold value of 17 (i.e., the average number of monitoring sites in all prefectures). The prefectures that meet the threshold are indicated in purple. The figure is based on the results shown in Figs. 7 (e, f) and 8.

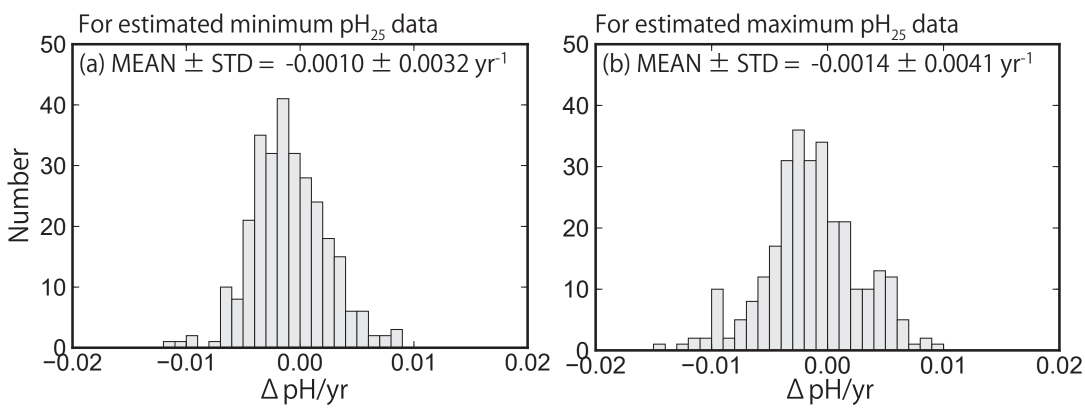

Fig. 10 Same as Fig. 7, but showing the pH_{25} trends at 289 sites (selected by quality control step 3). The value of pH_{25} was estimated using the method of Lui and Chen (2017).

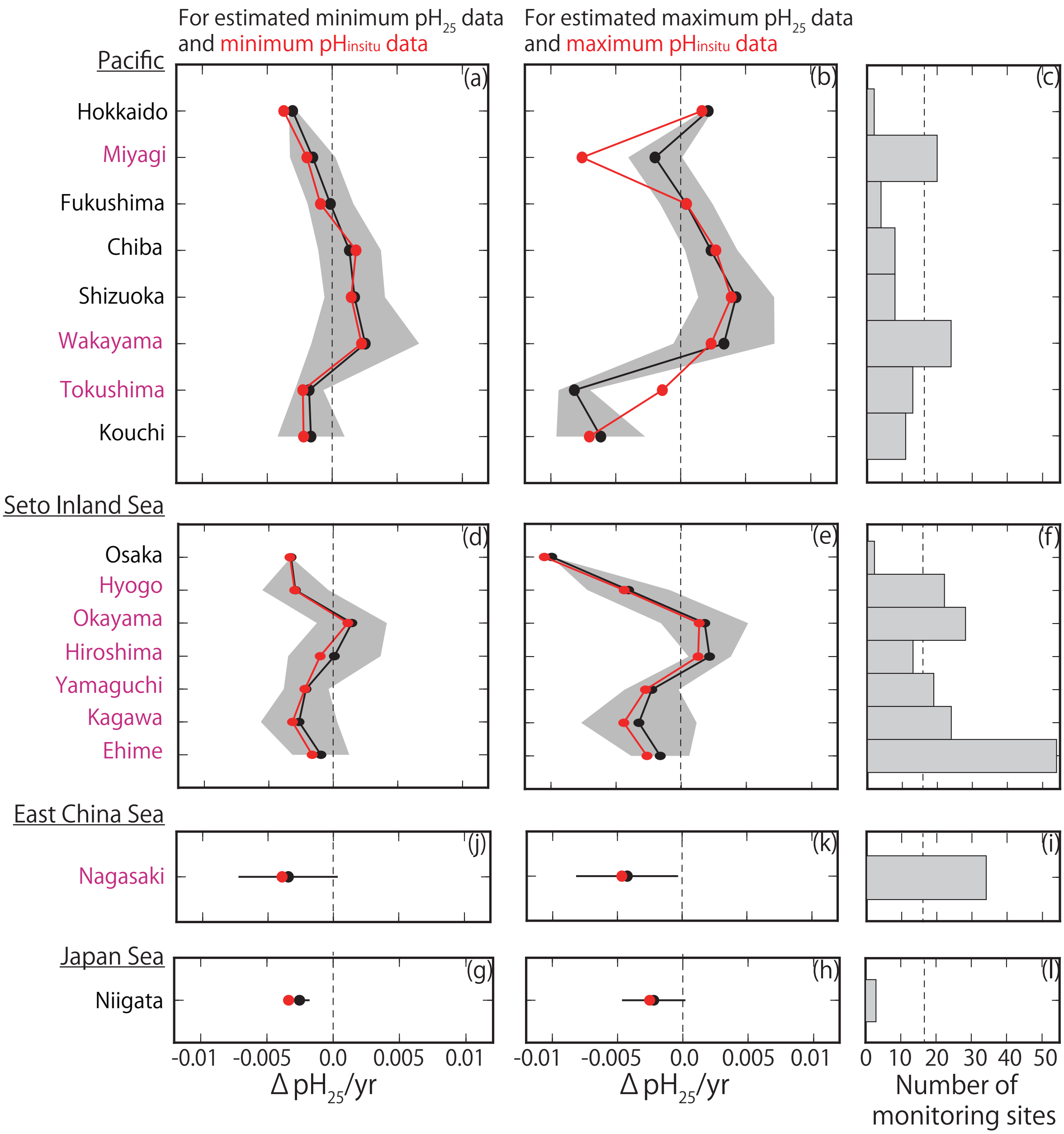

Fig. 11 (a–b, d–e, g–h, j–k) Same as Fig. 9, but showing the average estimated minimum and maximum pH_{25} trends (ΔpH_{25}/yr) for each prefecture. Red lines and points indicate the average minimum and maximum pH_{insitu} trends shown in Fig. 9.

Biogeosciences Discuss., https://doi.org/10.5194/bg-2019-150
Manuscript under review for journal Biogeosciences
Discussion started: 21 May 2019

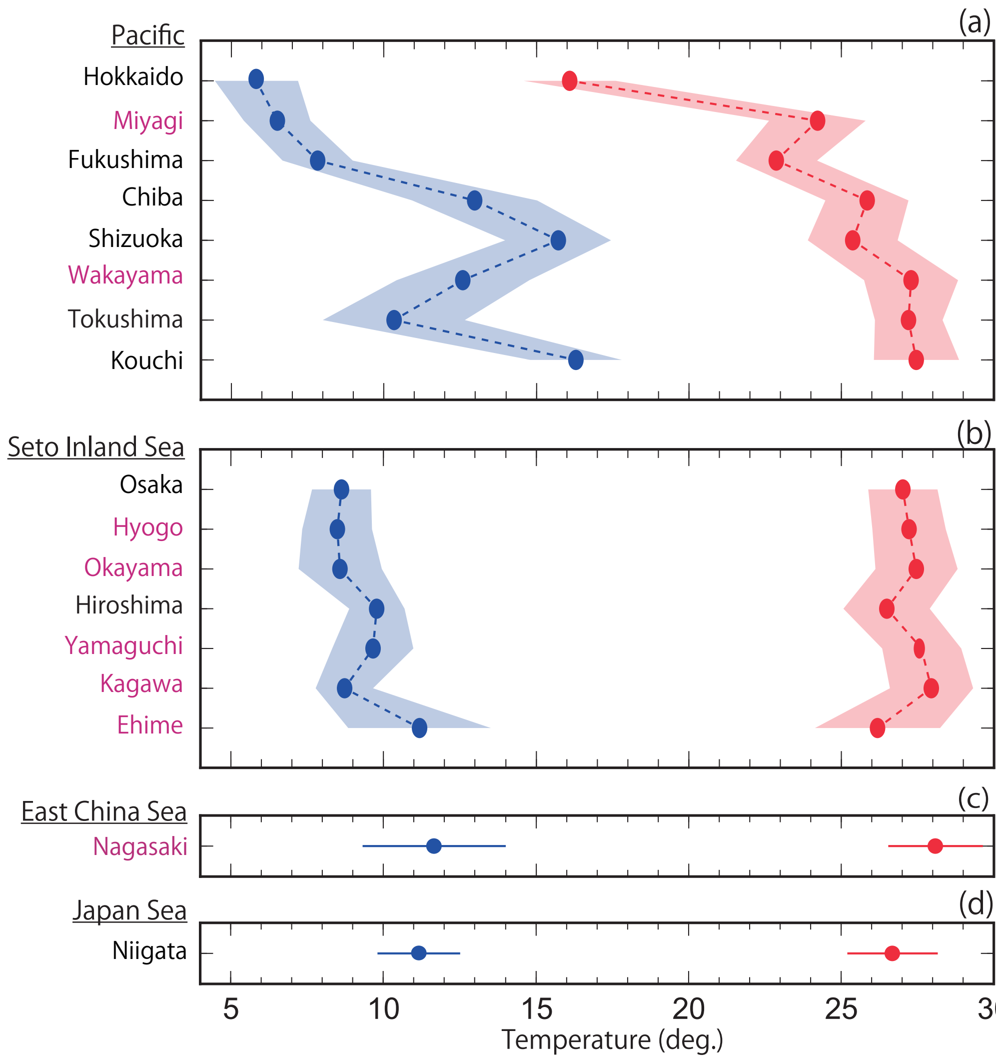

Fig. 12 Average highest and lowest temperatures observed for the minimum and maximum pH_{insitu} data for each prefecture. The blue and red lines and shading indicate the average and one standard deviation from the average, respectively. The prefectures that met the threshold of 17 are shown in purple, as in Figs. 9 (c-l) and 11 (c-l).

Biogeosciences Discuss., https://doi.org/10.5194/bg-2019-150
Manuscript under review for journal Biogeosciences
Discussion started: 21 May 2019

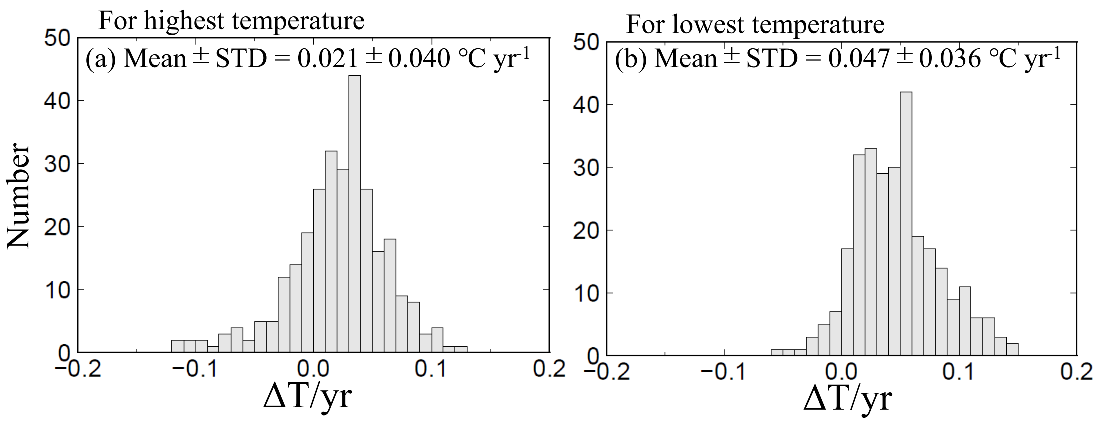

Fig. 13 Same as Fig. 7, but showing the highest and lowest temperature trends at 289 sites (selected by quality control step 3).

Biogeosciences Discuss., https://doi.org/10.5194/bg-2019-150
Manuscript under review for journal Biogeosciences
Discussion started: 21 May 2019

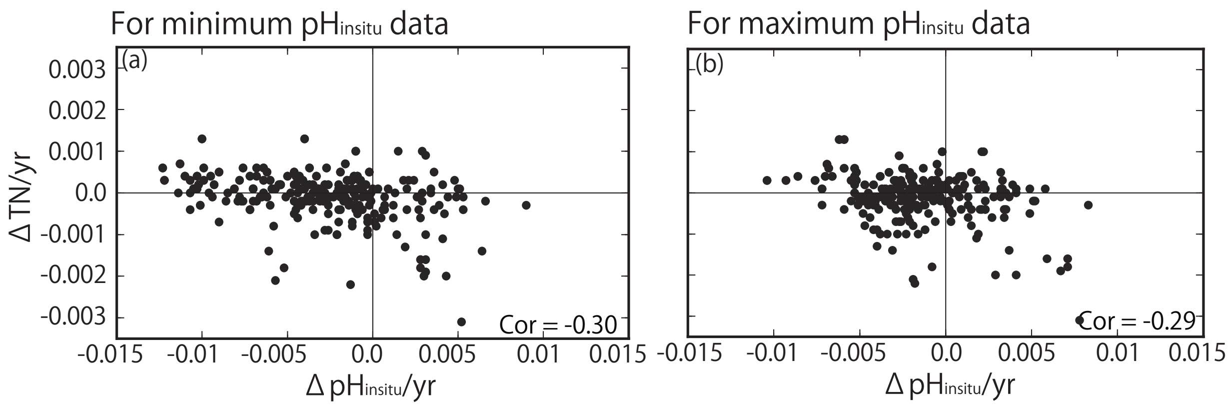

Fig. 14 Correlation between trends in total nitrogen (TN) and trends in (a) minimum and (b) maximum pH_{insitu}. The correlation coefficients are −0.30 and −0.29 for the minimum and maximum pH_{insitu}, respectively (significance level of 0.05, r = 0.128; degrees of freedom = 236).

Biogeosciences Discuss., https://doi.org/10.5194/bg-2019-150
Manuscript under review for journal Biogeosciences
Discussion started: 21 May 2019

Table 1 Number of samples (N) collected at each of the 1481 monitoring sites each year.

Year	0≦N＜4	4≦N＜8	8≦N＜12	12≦N＜16	16≦N＜20	20≦N＜24	24≦N＜28	28≦N＜32	32≦N＜40
1978	43	391	83	303	87	15	176	9	4
1979	31	372	73	328	101	19	150	11	7
1980	32	363	88	324	101	15	192	12	5
1981	24	347	72	361	99	13	199	11	3
1982	25	350	74	364	93	9	206	11	4
1983	32	355	75	356	91	11	222	12	0
1984	28	362	74	355	96	10	211	11	3
1985	24	354	86	377	96	9	192	11	8
1986	25	361	81	334	98	8	235	11	9
1987	26	357	78	341	98	4	239	11	1
1988	25	366	74	356	82	6	236	11	2
1989	26	365	83	344	84	5	238	17	3
1990	24	377	76	347	83	1	238	14	5
1991	24	367	80	355	93	5	226	13	5
1992	24	367	79	352	95	1	230	16	0
1993	17	374	76	357	94	8	225	14	0
1994	17	376	85	347	102	24	208	14	3
1995	29	376	109	311	104	3	227	12	0
1996	19	419	80	307	104	4	226	14	1
1997	20	396	82	315	115	5	225	13	0
1998	16	389	103	325	99	0	225	12	0
1999	17	396	68	381	67	2	224	12	7
2000	17	389	82	376	72	1	231	6	2
2001	17	392	90	382	50	8	220	6	1
2002	17	368	102	392	49	1	229	7	0
2003	17	365	93	402	51	1	233	6	1
2004	17	370	84	400	50	1	240	5	2
2005	16	354	152	356	46	9	228	3	0
2006	16	370	134	345	50	0	244	5	3
2007	17	399	128	353	62	0	202	5	3
2008	17	402	128	350	64	0	211	5	1
2009	17	403	143	340	58	0	217	5	8

Biogeosciences Discuss., https://doi.org/10.5194/bg-2019-150
Manuscript under review for journal Biogeosciences
Discussion started: 21 May 2019

Table 2 Average mutual correlation coefficients among water temperatrue and pH_{insitu} at adjacent monitoring sites in the same prefecture. The averages were calculated from the data for the highest and lowest temperature, and minimum and maximum pH_{insitu} within 15 km for the three criteria. We refined the sites using three quality control steps, yielding 1481 (step 1), 1127 (step 2), and 302 (step 3) sites.

Quality check procedue	highest temperature data	lowest temperature data	minimum pH_{insitu} data	maximum pH_{insitu} data
1	0.79	0.78	0.51	0.64
2	0.8	0.79	0.54	0.69
3	0.85	0.87	0.62	0.72

Table 3 Average correlation coefficients between minimum and maximu pHi_{nsitu} trends and total inorganic nitrogen (TN) ones, respectively. We evaluated this for the data after each quality check procedues. Degree of freedom in step 1 and 2 are same values, because TN data are not necessarily measured at the whole of pH_{insitu} monitoring sites. The sampling number of monitoring sites at step 1 and 2 were therefore the same number. Significant level, α = 0.05 and degree of freedom are also represented.

Quality check procedue	Correlation between minimum Δ pHinsitu and ΔTN	Correlation between maximum Δ pHinsitu and ΔTN	Significant level of 0.05	Degree of freedom
1	-0.015	-0.29	0.08	622
2	-0.015	-0.29	0.08	622
3	-0.33	-0.35	0.14	215